Chapter 12

Structure of Amorphous Materials

Chapter Outline

12.1. PDF ANALYSIS OF AMORPHOUS MATERIALS

Historically, the PDF technique was used predominantly for the structural study of amorphous materials, as briefly mentioned in Section 3.1.4. However, the advent of synchrotron-based radiation sources which enabled the application of the PDF technique to crystalline materials has also impacted the study of amorphous materials. Termination errors, which have been a major source of uncertainty for the PDF analysis of liquids and glasses for a long time, are now minimized because of the use of high-energy X-rays and neutrons which greatly extended the Q range. High intensities of the sources and the use of 2D X-ray and neutron detectors very significantly reduce statistical noise. Consequently, more detailed studies are now done routinely, including the analysis of anisotropic amorphous structures,

Pergamon Materials Series, Vol. 16. http://dx.doi.org/10.1016/B978-0-08-097133-9.00012-5

making PDF measurements more relevant to the understanding of the complex physical phenomena of glasses and liquids. In earlier days, the only quantities that could be reliably deduced from the PDF data of amorphous materials were the average distance to the nearest neighbors (position of the first peak of the PDF) and the coordination number (area of the first peak of the RDF). Today, more detailed information regarding the local atomic environment, represented, for instance, by the shape of the first peak, medium-range order characterized by higher order peaks, and the use of differential PDF methods, is garnered from accurate PDF measurements. In particular, the use of 2D X-ray detectors made it possible to determine the anisotropic PDF (Section 3.4.2) with much higher accuracy than before. These data are having a big impact on the study of metallic glasses and the understanding of the physics of glasses as reviewed below.

12.2. STRUCTURE OF MULTICOMPONENT GLASSES

12.2.1. Compositionally Resolved Structure

Except for few examples such as amorphous silicon, most stable glasses have two or more chemical components. In the case of metallic glasses, it is known that destabilizing solid solution by alloying elements with sufficient size differences leads to glass formation (Egami and Waseda, 1984). To describe the structure of multicomponent systems, ideally we need to know the compositionally resolved partial structure (Section 3.1.5). However, it is extremely challenging to determine experimentally all the partial structures with sufficient accuracy. In particular, real glasses contain more than two components. For an n-component system, we need to know $n(n+1)/2$ partial structures, but determining all the partial structures for such a multicomponent system is practically impossible.

On the other hand, the differential PDF, the PDF from a particular element to all others (Section 3.2.1), can be determined with reasonable accuracy using anomalous X-ray scattering (Section 3.2.2; Fig. 12.1) or isotope substitution for neutron scattering (Section 3.2.3), and generally, it provides sufficient information about the chemical environment. Combining the differential PDF with careful modeling, including the Reverse Monte Carlo (RMC) technique (McGreevy and Pusztai, 1988), is the best way to assess the real structure of the glass. To determine the nearest neighbor environment, the differential PDF could be substituted by the EXAFS PDF (Appendix 3.4). The EXAFS PDF coupled with the first-principles calculations proved to be a powerful tool in determining the local structure of metallic glasses (Sheng *et al.*, 2006). It should be noted that to construct a model with the RMC directly from the total PDF alone is extremely dangerous. The RMC tends to choose the most random structure, so unless some constraints are imposed, it severely underestimates the chemical short-range order. At the same time, choosing the constraints is also rife with hazard, because by changing the constraints, one can get almost any

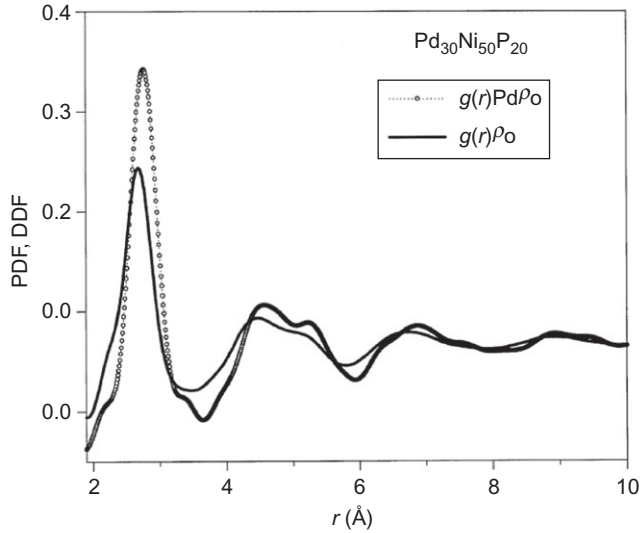

FIGURE 12.1 Differential PDF (DDF) from palladium (circles) and the total PDF (solid line) for glassy $Pd_{30}Ni_{50}P_{20}$ determined by the anomalous X-ray diffraction in the vicinity of the Pd K-edge (Egami *et al.*, 1998).

results one wants. Thus, obtaining the differential PDF, or the EXAFS PDF, is a minimum requirement in determining the structure of a multicomponent glass. It should be complemented by careful modeling, including the first-principles calculations.

12.3. STRUCTURAL CHANGES DUE TO STRUCTURAL RELAXATION

12.3.1. Structural Relaxation in Glasses

The structure of a crystal is well defined and does not change with temperature except for thermal expansion, unless a phase transformation intervenes. The structure of a liquid, on the other hand, is not well defined and is dynamically fluctuating. Furthermore, the average structure of a liquid actually changes with temperature. Indeed there are numerous evidences that the atomic structure of a liquid is temperature dependent. The specific heat of a liquid is well in excess of the Dulong–Petit law of $3k_B$ per atom, reflecting the configurational enthalpy necessary for the structural change. In effect, a liquid is undergoing a continuous phase transformation from highly disordered structures at high temperatures to structures with higher degrees of short-range order at lower temperatures. The viscosity of a liquid, η, changes rapidly with temperature, from 10^{13} poise at the glass transition by definition to centipoises above the melting temperature. If we express the temperature dependence of viscosity in terms of the apparent activation energy, E_a, by $\eta(T) = \eta_0 \exp(E_a/k_BT)$, E_a strongly depends

on temperature and decreases with increasing temperature. This is yet another piece of evidence that the structure of a liquid is temperature dependent.

When a liquid is cooled to a temperature below the glass transition temperature, T_g, a glass is formed. The structure of a glass depends on how fast the liquid was cooled, because faster cooling will freeze the structure of the liquid at a higher temperature. In fact, the glass obtained by extremely fast cooling in computer simulation, called the inherent structure (Sastry *et al.*, 1998), retains the topology of the structure (atomic connectivity) from which the liquid was cooled. The temperature at which the structure of a glass was in equilibrium in the liquid state is called the fictive temperature, T_f.

Thus, when a glass is obtained by fast cooling, the structure of the glass is not stable, and when it is held (annealed) at a temperature below T_g, the structure will relax into a more stable structure, a process called structural relaxation. During structural relaxation, almost all the properties of the glass change, to a varying extent (Chen, 1980; Egami, 1981). For instance, it is common that the volume decreases by up to half a percent. Because of this volume decrease, the structural relaxation is often described as the process of eliminating the excess "free volume." The free-volume theory proposed by Cohen and Turnbull (1959) has been successful in describing the temperature dependence of atomic transport in the hard-sphere systems and the systems with van der Waals interaction. However, in metallic systems, the interatomic potentials are more harmonic, and the free-volume theory is less successful (Egami, 2010) as Cohen and Turnbull warned in their original paper (1959). It is more appropriate to consider both positive and negative density fluctuations in describing the structural changes in metallic glasses (Egami *et al.*, 1981) rather than the free volume which corresponds to negative local density change. During structural relaxation, both positive and negative extremes of local density fluctuations are eliminated, resulting in a narrower density distribution (Kohda *et al.*, 2010).

12.3.2. Structural Relaxation Observed by the PDF Method

The changes in the PDF due to structural relaxation are small, but are observable. Generally, changes observed in the PDF under controlled conditions are much more reliable than the PDF itself, because many errors which degrade the accuracy of the PDF cancel themselves when the changes in the PDF are observed maintaining the identical experimental conditions on the same sample. The first observation of the changes in the PDF due to structural relaxation using energy-dispersive X-ray diffraction (Egami, 1978) already provided critical information on the nature of the relaxation phenomenon (Fig. 12.2). For instance, the relaxation is not incipient crystallization, but is a totally distinct phenomenon of approaching a more stable state within the glassy phase. In the free-volume picture, the system shrinks during the relaxation so that the changes in the PDF may be proportional to the first derivative

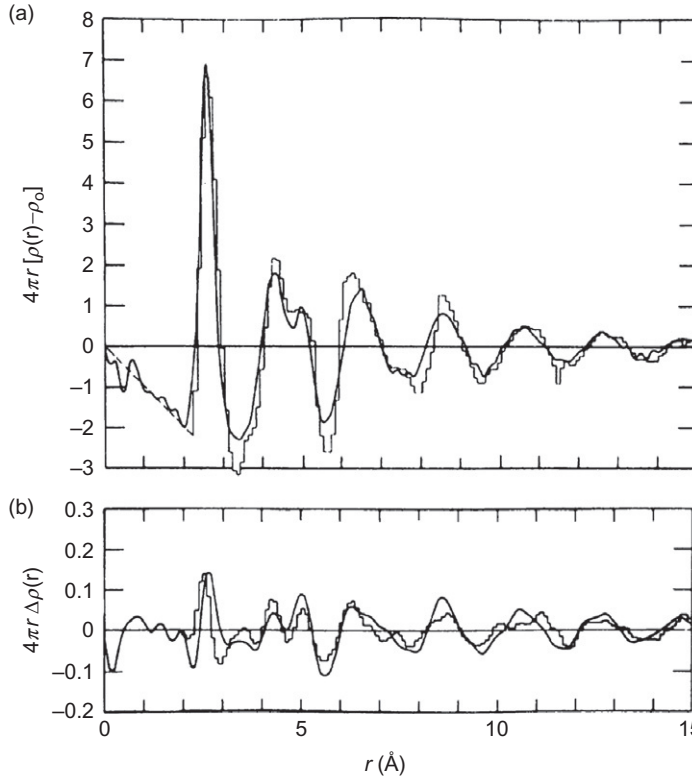

FIGURE 12.2 Change in the PDF of amorphous $Fe_{40}Ni_{40}P_{14}B_6$ due to structural relaxation (full line) (Egami, 1978) and the model calculation assuming the reduction in local density fluctuations (histogram) (Srolovitz *et al.*, 1981).

of the PDF. Instead, the observed changes are proportional to the second derivative of the PDF, which is more compatible with the idea of reducing both positive and negative local density fluctuations as shown by the histogram in Fig. 12.2 (Srolovitz *et al.*, 1981). Since then, the results were reproduced using modern tools of 2D detectors and synchrotron radiation (Dmowski *et al.*, 2007).

12.4. STRUCTURAL CHANGES DUE TO MECHANICAL DEFORMATION

12.4.1. Elastic Deformation

The mechanical strains in crystalline materials can readily be determined from the shifts in the position of the Bragg peaks (Warren, 1990). It was proposed that strains in glasses could be determined in the same way from the shifts in

$S(Q)$ (Poulsen *et al.*, 2004). Even though this may appear to be a simple and correct proposition, the reality actually is more complex. For a simple crystalline lattice (Bravais lattice), the elastic deformation is described by affine deformation,

$$\boldsymbol{r}' = (1 + \bar{\bar{\varepsilon}})\boldsymbol{r}, \tag{12.1}$$

where $\boldsymbol{r}$ and $\boldsymbol{r}'$ describe the atomic positions before and after deformation, respectively, and $\bar{\bar{\varepsilon}}$ is the strain tensor. However, if the unit cell has two atoms, they may not move exactly in the same manner, so we need two strain tensors,

$$\boldsymbol{r}_\alpha{}' = (1 + \bar{\bar{\varepsilon}}_\alpha)\boldsymbol{r}_\alpha, \quad \alpha = 1, 2, \tag{12.2}$$

where α indexes the atom in the unit cell. Amorphous materials have no periodicity, so they are like a crystal with an infinitely large unit cell, in which every atom behaves differently. Therefore, elastic deformation in a glass cannot be described by affine deformation (Weaire *et al.*, 1971). Moreover, simulations showed that some topological changes in the atom connectivity network, such as the changes from the nearest neighbor to the second nearest neighbor, take place even in the seemingly linear, thus apparently elastic region (Suzuki and Egami, 1985). In metallic glasses, the interatomic potentials have a negative curvature in the region between the first and second peaks of the PDF because of Friedel oscillations (Hafner *et al.*, 1987). Thus, a pair of atoms, whose interatomic distance is within the first PDF peak but close to the valley, can move significantly with a small stress such that their interatomic distance falls to the second peak after the move. If we define the "metallic bond" by atoms being the nearest neighbor, then a small stress can cut some weak bonds and create topological changes to the local structure.

After elastic deformation, the structure is no longer isotropic, so we have to use the anisotropic PDF method to describe such a structure. Often researchers measure $S(Q)$ in two directions, parallel and perpendicular to the stress, and then apply the usual sine Fourier transform, Eq. (3.1). However, this procedure is not justified because Eq. (3.1) was derived assuming an isotropic structure. Instead, one should apply the full anisotropic PDF analysis with the spherical Bessel transformation as explained in Section 3.4.2 and Appendix 3.5. Examples of the isotropic and anisotropic structure function and PDF of a deformed metallic glass are shown in Figs. 12.3 and 12.4 (Dmowski *et al.*, 2010a). In this case, uniaxial stress of up to 1.2 GPa, which is below the apparent elastic limit, was applied on glassy $Zr_{52.5}Cu_{17.9}Ni_{14.6}Al_{10}Ti_5$. The measurement was made with synchrotron X-rays of 120 keV using a 2D detector. The anisotropic PDF is close to the PDF expected for affine deformation as shown in Fig. 12.5, but clear deviations are seen at short distances, indicating that the apparently elastic deformation has significant nonaffine components, as suggested by simulations.

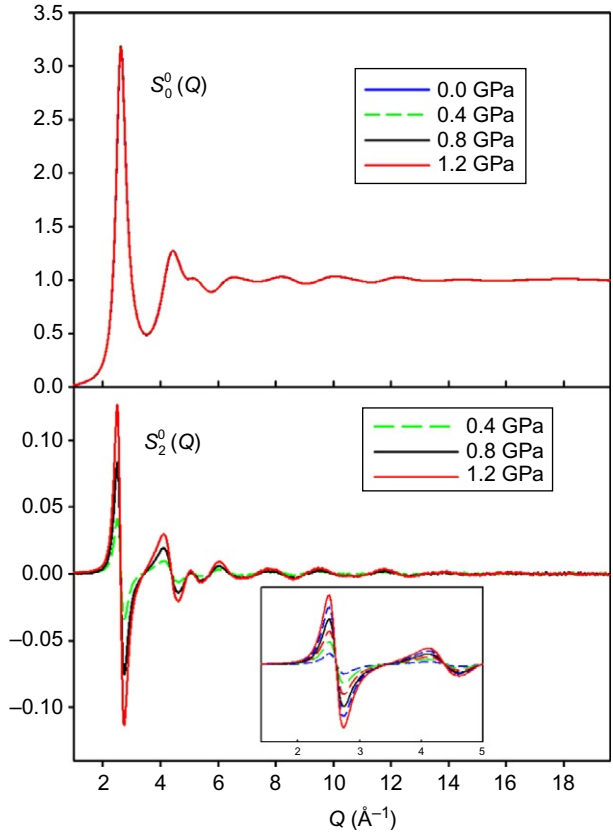

FIGURE 12.3 Isotropic and anisotropic structure function, $S_0^0(Q)$ and $S_2^0(Q)$, for a metallic glass under uniaxial tensile stress up to 1.2 GPa. In the inset, the applied stresses are from 0.2 to 1.2 GPa with a step of 0.2 GPa (Dmowski *et al.*, 2010a).

12.4.2. Anelastic Deformation

Using modern tools of synchrotron X-ray with 2D detectors, the anisotropic PDF due to anelastic creep deformation (Fig. 3.12) was determined with higher accuracy (Fig. 12.6, Dmowski *et al.*, 2010a). The result is compared to the PDF expected for affine deformation. They agree at large distances, but again, significant deviations are seen at short distances. However, the deviations are similar to those in Fig. 12.5, except much larger in amplitude. This suggests that metallic glasses under apparently elastic deformation contain a significant anelastic component, as also suggested by simulation (Suzuki and Egami, 1985). Indeed, the anisotropic PDF shown in Fig. 12.4 can be fitted with the sum of the PDF for affine deformation and the PDF for creep deformation (Dmowski *et al.*, 2010a).

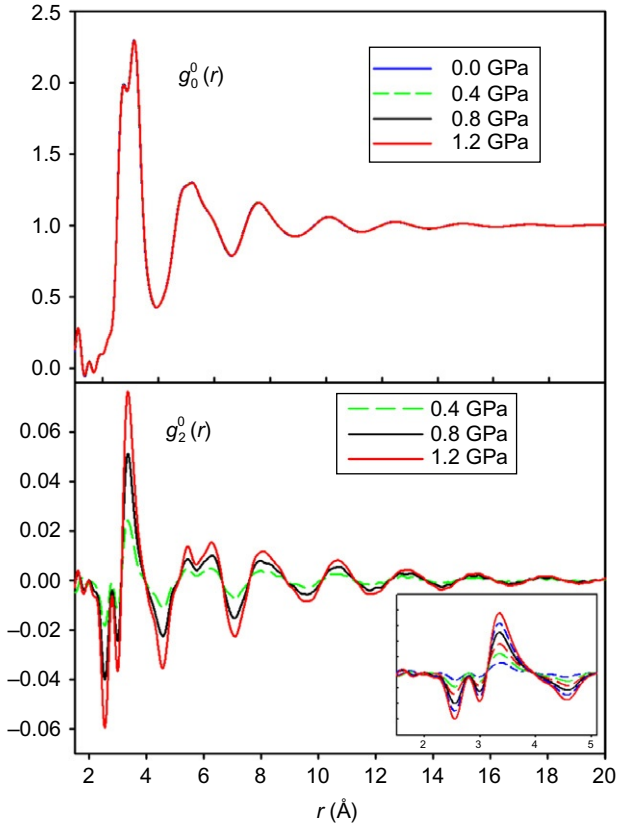

FIGURE 12.4 Isotropic and anisotropic PDF, $g_0^0(r)$ and $g_0^2(r)$, for a metallic glass under uniaxial tensile stress up to 1.2 GPa. In the inset, the applied stresses are from 0.2 to 1.2 GPa with a step of 0.2 GPa (Dmowski *et al.*, 2010a).

The anisotropic PDF due to anelastic creep deformation (Figs. 3.12 and 12.6) was interpreted in terms of bond-orientational anisotropy (BOA) induced by bond-exchange processes such as those in Fig. 3.13 (Suzuki *et al.*, 1987; Tomida and Egami, 1995). Topological deviations from the isotropic structure such as BOA retain a memory of the sample's heat treatment under stress and cause the anelastic effect. When the system is annealed without stress, the anisotropy slowly disappears.

12.4.3. Plastic Deformation

Most glasses, such as oxide glasses, are brittle and fracture without plastic deformation. Metallic glasses are exceptions, and many of them show some plastic deformation at least in compression. But the atomistic mechanism of

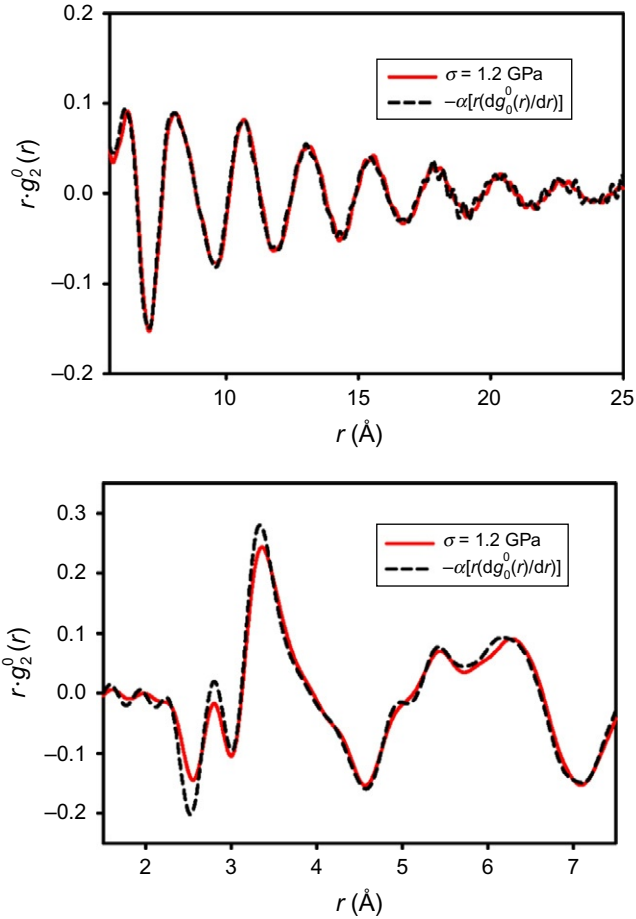

FIGURE 12.5 The anisotropic PDF, $g_2^0(r)$, under 1.2 GPa (red line) compared to the result expected for affine deformation (dashed line) (Dmowski *et al.*, 2010a).

plastic deformation in metallic glasses is a hotly debated, yet still unresolved, issue. Crystals deform plastically due to the motion of dislocations. However, in glasses, which lack a periodic lattice, dislocations cannot be defined. Earlier proposals include the free-volume model (Spaepen, 1977) and the distributed free-volume model (Argon, 1979). Both of these models involve local dilatation to create free volume, implying that deformation should be sensitive to pressure. However, experimental results on metallic glasses suggest that the mechanical strengths for tensile and compression tests are very similar, and thus the effect of pressure on fracture is small (Varadarajan and Lewandowski, 2010). In addition, simulations show that pure shear, without involving change in volume, can induce a glass transition (Guan *et al.*,

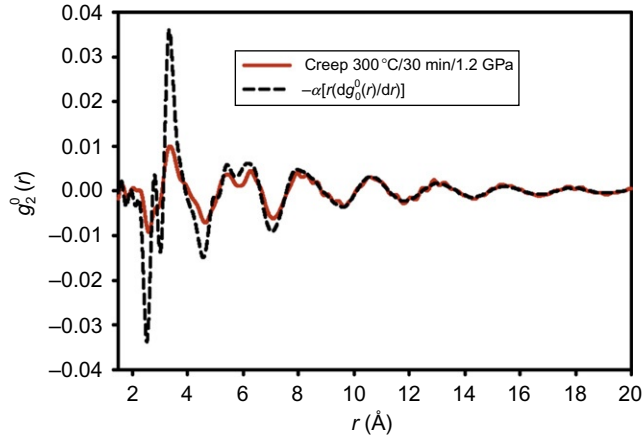

FIGURE 12.6 The anisotropic PDF, $g_2^0(r)$, after creep at 300 °C under 1.2 GPa for 30 min (red line) compared to the result expected for affine deformation (dashed line) (Dmowski *et al*., 2010a).

2010). The leading model today is the shear transformation zone (STZ) model in which some collective shear deformation occurs locally (Falk and Langer, 1998; Langer, 2004). However, the size of the STZ and other details are still controversial (Johnson and Samwer, 2007).

Metallic glasses deform plastically forming many very thin slip bands (Masumoto and Maddin, 1971; Spaepen, 1977; Zhang and Greer, 2006), and plastic deformation is localized within these bands. Because the volume fraction of the shear bands in the sample is small, it is not easy to determine directly the atomic structure within the band (Donovan and Stobbs, 1981). In addition, shear bands become heated because of the work done by deformation (Lewandowski and Greer, 2006; Nieh and Liaw, 2006), and most likely transform into a liquid (Spaepen, 2006). As a consequence, any structural signature of mechanical deformation will be wiped out by melting, in the "perfect crime syndrome." What is observed in heavily plastically deformed metallic glasses is the evidence of "rejuvenation," the opposite of structural relaxation created as a result of melting and subsequent very rapid cooling (Dmowski *et al*., 2010b). It is most likely that plastic deformation occurs as a result of percolation of many anelastic deformation centers, and the STZ should be identified with the anelastic deformation centers, but the proof of this speculation has not been attained yet.

REFERENCES

Argon, A.S. (1979) *Acta Metall*., **27**, 47.
Chen, H.S. (1980) *Rep. Prog. Phys*., **43**, 353.
Cohen, M.H. & Turnbull, D. (1959) *J. Chem. Phys*., **31**, 1164.

Dmowski, W., Fan, C., Morrison, M.L., Liaw, P.K. & Egami, T. (2007) *Mater. Sci. Eng. A*, **471**, 125.
Dmowski, W., Iwashita, T., Chuang, A., Almer, J. & Egami, T. (2010a) *Phys. Rev. Lett.*, **105**, 205502.
Dmowski, W., Yokoyama, Y., Chuang, A., Ren, Y., Umemoto, M., Tuchiya, K., Inoue, A. & Egami, T. (2010b) *Acta Mater.*, **58**, 429.
Donovan, P.E. & Stobbs, W.M. (1981) *Acta Metall.*, **29**, 1419.
Egami, T. (1978) *J. Mater. Sci.*, **13**, 2587.
Egami, T. (1981) *Ann. N. Y. Acad. Sci.*, **37**, 238.
Egami, T. (2010) *J. Met.*, **62**(2), 70.
Egami, T. & Waseda, Y. (1984) *J. Non-Cryst. Solids*, **64**, 113.
Egami, T., Maeda, K., Srolovitz, D. & Vitek, V. (1981) *J. Phys.*, **41**, C8–C272.
Egami, T., Dmowski, D., He, Y. & Schwarz, R. (1998) *Metall. Mater. Trans.*, **29A**, 1805.
Falk, M. & Langer, J.S. (1998) *Phys. Rev. E*, **57**, 7192.
Guan, P., Chen, M.-W. & Egami, T. (2010) *Phys. Rev. Lett.*, **104**, 205701.
Hafner, J., Egami, T., Aur, S. & Giessen, B.C. (1987) *J. Phys. F*, **17**, 1807.
Johnson, W.L. & Samwer, K. (2007) *Phys. Rev. Lett.*, **95**, 195501.
Kohda, M., Haruyama, O. & Egami, T. (2010) *Phys. Rev. B*, **81**, 092203.
Langer, J.S. (2004) *Phys. Rev. E*, **70**, 041502.
Lewandowski, J.J. & Greer, A.L. (2006) *Nat. Mater.*, **5**, 15.
Masumoto, T. & Maddin, R. (1971) *Acta Metall.*, **19**, 725.
McGreevy, R.L. & Pusztai, L. (1988) *Mol. Simul.*, **1**, 359.
Nieh, T.G. & Liaw, P.K. (2006) *J. Mater. Res.*, **21**, 915.
Poulsen, H.F., Wet, J.A., Neuefeind, J., Honkimäki, V. & Daymond, M. (2004) *Nat. Mater.*, **4**, 33.
Sastry, S., Debenedetti, P.G. & Stillinger, F.H. (1998) *Nature*, **393**, 554.
Sheng, H.W., Luo, W.K., Alamgir, F.M., Bai, J.M. & Ma, E. (2006) *Nature*, **439**, 419.
Spaepen, F. (1977) *Acta Metall.*, **25**, 407.
Spaepen, F. (2006) *Nat. Mater.*, **5**, 7.
Srolovitz, D., Egami, T. & Vitek, V. (1981) *Phys. Rev. B*, **24**, 6936.
Suzuki, Y. & Egami, T. (1985) *J. Non-Cryst. Solids*, **75**, 361.
Suzuki, Y., Haimovich, J. & Egami, T. (1987) *Phys. Rev. B*, **35**, 2162.
Tomida, T. & Egami, T. (1995) *Phys. Rev. B*, **52**, 3290.
Varadarajan, R. & Lewandowski, J.J. (2010) *Metall. Mater. Trans. A*, **41**, 1758.
Warren, B.E. (1990) *X-ray Diffraction*. New York: Dover.
Weaire, D., Ashby, M.F., Logan, J. & Weins, M.J. (1971) *Acta Metall.*, **19**, 779.
Zhang, Y. & Greer, A.L. (2006) *Appl. Phys. Lett.*, **89**, 071907.